

Diffusion of α -Tocopherol in Membrane Models: Probing the Kinetics of Vitamin E Antioxidant Action by Fluorescence in Real Time

Gabriela Gramlich,[†] Jiayun Zhang,[†] and Werner M. Nau^{*,†,‡}

Contribution from the Department Chemie, Universität Basel, Klingelbergstrasse 80, CH-4056 Basel, Switzerland, and School of Engineering and Science, International University Bremen, Campus Ring 1, D-28759 Bremen, Germany

Received November 28, 2003; E-mail: w.nau@iu-bremen.de

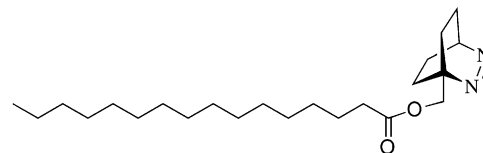
Abstract: The new fluorescent membrane probe Fluorazophore-L, a lipophilic derivative of the azoalkane 2,3-diazabicyclo[2.2.2]oct-2-ene, is employed to study the quenching of α -tocopherol (α -Toc) by time-resolved fluorescence in the microheterogeneous environments of Triton XR-100 and SDS micelles, as well as POPC liposomes. Fluorazophore-L has a small nonaromatic fluorescent polar headgroup and an exceedingly long-lived fluorescence (e.g., 140 ns in aerated SDS micelles), which is efficiently quenched by α -Toc ($3.9 \times 10^9 \text{ M}^{-1} \text{ s}^{-1}$ in benzene). Based on solvatochromic effects and the accessibility by water-soluble quenchers, the reactive headgroup of Fluorazophore-L, along with the chromanol group of α -Toc, resides at the water–lipid interface, which allows for a diffusion-controlled quenching in the lipidic environments. The quenching experiments represent an immobile or stationary case; that is, interparticle probe or quencher exchange during the excited-state lifetime is insignificant. Different quenching models are used to characterize the dynamics and antioxidant action of α -Toc in terms of diffusion coefficients or, where applicable, rate constants. The ideal micellar quenching model is suitable to describe the fluorescence quenching in SDS micelles and affords a pseudo-unimolecular quenching rate constant of $2.4 (\pm 0.4) \times 10^7 \text{ s}^{-1}$ for a single quencher per micelle along with a mean aggregation number of 63 ± 3 . In Triton micelles as well as in unilamellar POPC liposomes, a two-dimensional (lateral) diffusion model is most appropriate. The mutual lateral diffusion coefficient D_L for α -Toc and Fluorazophore-L in POPC liposomes is found to be $1.8 (\pm 0.1) \times 10^{-7} \text{ cm}^2 \text{ s}^{-1}$, about a factor of 2 larger than for mutual diffusion of POPC, but more than 1 order of magnitude lower than a previously reported value. The comparison of the different environments suggests a quenching efficiency in the order benzene \gg SDS micelles $>$ Triton micelles $>$ POPC liposomes, in line with expectations from microviscosity. The kinetic measurements provide important benchmark values for the modeling of oxidative stress in membranes and other lipidic assemblies. The special case of small lipidic assemblies (SDS micelles), for which the net antioxidant efficacy of α -Toc may be lower than expected on the grounds of its diffusional behavior, is discussed.

Introduction

The azoalkane 2,3-diazabicyclo[2.2.2]oct-2-ene (DBO) has been introduced as a fluorescent probe for antioxidants in solution.^{1,2} Its strongly fluorescent n,π^* -excited state shows radical-like behavior and is quenched with high efficiency and selectivity by antioxidants through hydrogen atom abstraction. Due to the exceedingly long fluorescence lifetime of DBO (e.g., 325 ns in aerated water), sizable quenching effects result at physiologically relevant concentrations of chain-breaking antioxidants (micromolar to millimolar).¹ The fluorescence quenching can be temporally resolved with high sensitivity, allowing a direct and accurate kinetic analysis of the primary redox reactions of antioxidants.^{3,4}



DBO



Fluorazophore-L

Recently, we have synthesized an amphiphilic DBO derivative, Fluorazophore-L, in which the characteristic reactivity and long lifetime are retained.⁵ In a preliminary communication, we established Fluorazophore-L as a mimic of reactive membrane radicals, in the investigation of interfacial phenomena with the water-soluble vitamin C.⁶ Now, we report the application of its

[†] Universität Basel.

[‡] International University Bremen.

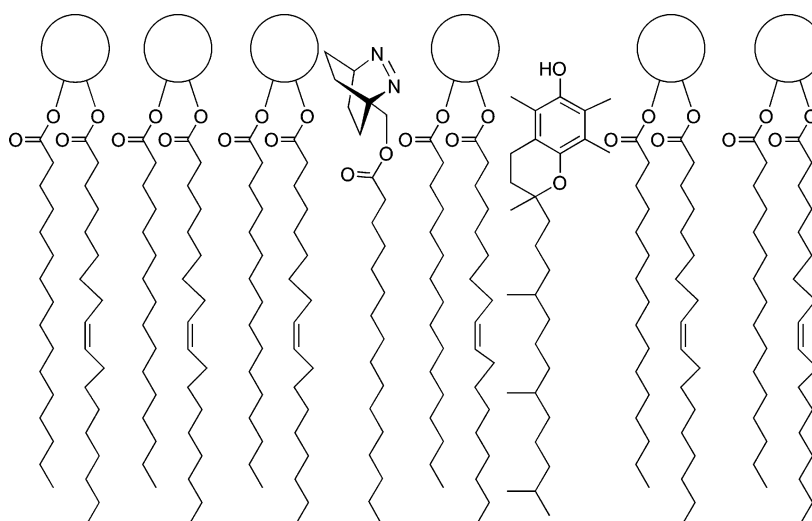
(1) Nau, W. M. *J. Am. Chem. Soc.* **1998**, *120*, 12614–12618.
 (2) Zhang, X.; Nau, W. M. *J. Inf. Rec.* **2000**, *25*, 323–330.
 (3) Zhang, X.; Erb, C.; Flammer, J.; Nau, W. M. *Photochem. Photobiol.* **2000**, *71*, 524–533.

(4) Erb, C.; Nau-Staudt, K.; Flammer, J.; Nau, W. M. *Ophthalmic Res.* **2004**, *36*, 38–42.

(5) Gramlich, G.; Zhang, J.; Winterhalter, M.; Nau, W. M. *Chem. Phys. Lipids* **2001**, *113*, 1–9.

(6) Gramlich, G.; Zhang, J.; Nau, W. M. *J. Am. Chem. Soc.* **2002**, *124*, 11252–11253.

Scheme 1



unique properties to study the antioxidant activity of α -tocopherol (α -Toc), the most active component of vitamin E,⁷ in membrane models and micelles. As illustrated in Scheme 1, both amphiphilic reaction partners have their reactive headgroups positioned at the lipid/water interface, which allows for an efficient fluorescence quenching upon diffusive encounter. By this methodology, we can mimic an antioxidant–prooxidant interaction in membranes, follow the kinetics of this reaction by time-resolved fluorescence, and determine the diffusion coefficients. To the best of our knowledge,⁸ this is the first study in which the interception of a reactive species by α -Toc as an antioxidant is directly monitored in real time in phospholipid membrane models.

Materials and Methods

Fluorazophore-L was synthesized as reported.⁵ All solvents used were of spectroscopic-grade purity (Fluka). Water was bidistilled. The buffer used for liposome preparations contained 26 mM KH_2PO_4 and 41 mM Na_2HPO_4 (Titrisol pH 7.0, from Merck). 1-Palmitoyl-2-oleoyl-*sn*-glycero-3-phosphocholine (POPC) was obtained as powder from Avanti Polar Lipids (Birmingham, AL) and dried to a monohydrate in the presence of P_4O_{10} under high-vacuum prior to use.⁹ DL- α -Tocopherol (>98%), sodium dodecyl sulfate (SDS, MicroSelect), and *t*-octyl-cyclohexylpolyethoxyethanol (Triton XR-100) were purchased from Fluka. Triton XR-100 is the reduced form of Triton X-100 and contains a cyclohexyl instead of a phenyl ring, resulting in a lower absorption and fluorescence while preserving its detergent properties.¹⁰ SDS was purified by recrystallization from methanol.

The micelle solutions were freshly prepared by addition of neat Fluorazophore-L (1 mM bulk concentration) to the surfactant solutions with bulk concentrations of 100 mM for SDS and 27 mM for Triton XR-100. These are well above the critical micelle concentrations (cmc), which have been reported to be 8.0 mM for SDS^{11,12} and 0.25 mM for

Triton XR-100.¹⁰ The solutions were stirred overnight at 40 °C. α -Toc (0.1–0.5 M in ethanol) was added directly by injections to the Fluorazophore-L-labeled surfactant solution with a Hamilton syringe. These mixtures were stirred for 15 min at 40 °C and for 10 min at ambient temperature. The total amount of ethanol was below 0.8% and 0.2% for Triton XR-100 and SDS micelles, respectively.

The injection method^{13–16} was used to obtain medium-sized liposomes. Ethanolic solutions of POPC and Fluorazophore-L were mixed in a lipid-to-probe molar ratio of 10:1 to afford a stock solution with a concentration of 30 mM POPC and 3 mM fluorophore. To 84 μL of this solution was added 16 μL of ethanol containing various amounts of α -Toc. From the resulting POPC/probe/quencher mixture, 84 μL was directly injected through a Hamilton syringe into 3 mL of a magnetically stirred phosphate buffer (pH 7.0) at 40 °C. The resulting liposome dispersion, which has a final lipid concentration of 0.7 mM and an overall ethanol concentration of 2.2%, was stable for several hours, as monitored by light scattering. This was sufficiently long for the fluorescence experiments, which were carried out with freshly prepared samples. The small amounts of ethanol present in the system are not expected to cause a significant fluidizing effect on the liposomes.¹⁷

The dynamic light-scattering experiments were done under a scattering angle of 90° with an ALV-Langen goniometer equipped with a Nd:YAG laser ($\lambda = 532$ nm) and an ALV-5000/E correlator. UV absorption spectra were obtained with a Perkin-Elmer Lambda 19 spectrophotometer. The fluorescence decays were recorded with a time-correlated single-photon counting (SPC) fluorometer (FLS920, Edinburgh Instruments) and a PicoQuant diode laser LDH-P-C 375 ($\lambda_{\text{exc}} = 373$ nm, fwhm ca. 50 ps, $\lambda_{\text{obs}} = 450$ nm) for excitation. The laser pulse frequency was set below 2% of the inverse lifetime, while the count rate was adjusted to be not more than 2% of the laser frequency. The time for the SPC experiments was kept constant for each series, but sufficiently long to obtain 10^4 counts in the maximum after background subtraction. Steady-state fluorescence spectra ($\lambda_{\text{exc}} = 377$ nm) were also recorded with the FLS 920 setup.

The SPC measurements were performed with the respective sample, an identically prepared reference solution without Fluorazophore-L to

- (7) Burton, G. W.; Ingold, K. U. *Acc. Chem. Res.* **1986**, *19*, 194–201.
 (8) Previous studies in SDS micelles (Evans, C. H.; Scaiano, J. C.; Ingold, K. U. *J. Am. Chem. Soc.* **1992**, *114*, 140–146. Bisby, R. H.; Parker, A. W. *J. Am. Chem. Soc.* **1995**, *117*, 5664–5670) have involved α -Toc as a quencher of triplet states (butyrophenone or duroquinone) by using transient absorption and time-resolved Raman spectroscopy for detection. These investigations focused on the geminate radical recombinations involving α -tocopheroxyl radicals, the spectral characterization of the intermediates resulting from hydrogen abstraction, and the exit rates of the reduced probe radicals to the aqueous phase.
 (9) Feller, S. E.; Brown, C. A.; Nizza, D. T.; Gawrisch, K. *Biophys. J.* **2002**, *82*, 1396–1404.
 (10) Tiller, G. E.; Mueller, T. J.; Dockter, M. E.; Struve, W. G. *Anal. Biochem.* **1984**, *141*, 262–266.

- (11) Almgren, M.; Swarup, S. J. *Colloid Interface Sci.* **1983**, *91*, 256–266.
 (12) Cramb, D. T.; Beck, S. C. J. *Photochem. Photobiol., A* **2000**, *134*, 87–95.
 (13) Batzri, S.; Korn, E. D. *Biochim. Biophys. Acta* **1973**, *298*, 1015–1019.
 (14) Kremer, J. M. H.; Esker, M. W. J.; Pathmamanoharan, C.; Wiersma, P. H. *Biochemistry* **1977**, *16*, 3932–3935.
 (15) Baranyai, P.; Gangl, S.; Grabner, G.; Knapp, M.; Köhler, G.; Vidóczy, T. *Langmuir* **1999**, *15*, 7577–7584.
 (16) Domazou, A. S.; Luisi, P. L. *J. Liposome Res.* **2002**, *12*, 205–220.
 (17) Almeida, L. M.; Vaz, W. L. C.; Stimpel, J.; Madeira, V. M. C. *Biochemistry* **1986**, *25*, 4832–4839.

measure the background, and an empty cuvette ($\lambda_{\text{obs}} = \lambda_{\text{exc}}$) to obtain the instrument response function. The background signal was subtracted from the individual traces before data analysis; the latter was carried out according to the respective theoretical fluorescence decay kinetics. The program pro Fit 5.5.0 (QuantumSoft, Zürich) was used for the fitting of single decay traces as well as for global data analysis. Note that the probe lifetimes and quenching effects display a significant temperature dependence, presumably due to changes in the microviscosity of the medium, which requires a precise temperature control. This is particularly critical for POPC liposomes, for which the lifetime decreases, for example, from 125 ns at 24 °C to 116 ns at 27 °C. In all experiments, the temperature inside the cuvette was therefore kept constant at 27 ± 0.5 °C with a circulating water bath (Julabo F25/HD thermostat).

Care has to be taken to use the proper concentrations: $[Q]$, $[Q_{3D}]$, and $[Q_{2D}]$. $[Q]$ is the bulk concentration of quencher in units of mol per liter of total solution (including water); it was used in the calculation of the average number of quencher molecules per micelle. $[Q_{3D}]$ is the three-dimensional concentration based on the accessible volume within the lipidic assembly in units of mol of quencher per liter of lipid or surfactant; it was used in the Stern–Volmer analyses (see Supporting Information). The calculation of $[Q_{3D}]$ requires the “density” of the surfactants and lipids which was taken to be 1.029 g/mL for Triton XR-100, 1.15 g/mL for SDS,^{18,19} and 1.00 g/mL for POPC; the density of POPC can be derived from a reported molecular volume of 1267 Å³.²⁰ The two-dimensional concentration, $[Q_{2D}]$, of an amphiphilic quencher on the surface of a large micelle or liposome in units of molecules per cm² surface area was used to treat lateral diffusion. $[Q_{2D}]$ was calculated by taking the area per molecule as 70 Å² for POPC^{5,20} and 64 Å² for Triton XR-100 micelles.²¹ The calculation of $[Q_{2D}]$ assumes an ideal amphiphilic arrangement of the lipid and surfactant molecules within the self-assemblies, that is, with all headgroups positioned at the interface. This may be more strictly fulfilled for the unilamellar liposomes than for the less structured micelles.

The van der Waals radii of the headgroups were estimated to be 3.2 Å for the nearly spherical azo chromophore of Fluorazophore-L (AM1 calculations, this work)²² and 4.1 Å for the chromanol group of α -Toc.²³ They were consistent with the radii estimated from monolayer experiments,^{5,24} 3.3 Å for Fluorazophore-L and 3.8 Å for α -Toc.

Results

Photophysical Properties. UV absorption and fluorescence spectra of Fluorazophore-L in organic solvents closely resemble those of the parent DBO.⁵ The incorporation of Fluorazophore-L into micelles and phosphocholine liposomes is signaled by the solvatochromic effects characteristic of the change from an aqueous to a more hydrophobic solvent (Figure 1), which derive from a different polarizability of the environment.²⁵ The aqueous UV spectrum of the water-soluble DBO serves as a reference point ($\lambda_{\text{max}} = 365$ nm, $\epsilon = 45$ M⁻¹ cm⁻¹).^{26,27} The effect is least pronounced for inclusion into SDS micelles (0.1 M SDS) for which a slight bathochromic shift to 368 nm and an increased ϵ of 70 M⁻¹ cm⁻¹ was obtained, which is consistent with a positioning of the chromophore in a somewhat less polar, but

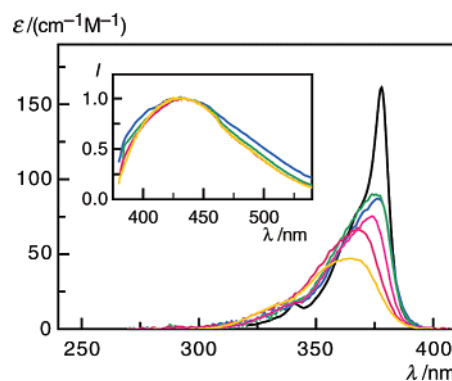


Figure 1. UV spectra of Fluorazophore-L in *n*-hexane (black), 27 mM Triton XR-100 (green), 1 mM POPC (blue), methanol (purple), 0.1 M SDS (red), and of the water-soluble DBO (yellow) in water. The inset shows the corresponding normalized fluorescence spectra with identical color codes.

still protic environment, presumably the water-rich interfacial Stern region.²⁸ In Triton XR-100 micelles and POPC liposomes, Fluorazophore-L gives a more distinct shift to 376 nm, a band sharpening, and, relative to DBO in water, a doubling of the extinction coefficient to ca. 90 M⁻¹ cm⁻¹. This solvatochromic effect is somewhat more pronounced than that in alcohols ($\lambda_{\text{max}} = 373$ nm, $\epsilon = 75$ M⁻¹ cm⁻¹ in methanol), but falls below that observed in hydrocarbons ($\lambda_{\text{max}} = 378$ nm, $\epsilon = 160$ M⁻¹ cm⁻¹ in *n*-hexane).⁵ The combined spectral data signal a location of the fluorophore in the outer region of the lipidic structure, close to the lipid/water interface. The very broad fluorescence spectrum of DBO has no distinct features and does not respond as strongly to environmental changes as the absorption spectrum.^{25,29} Accordingly, the fluorescence spectra of Fluorazophore-L in micellar and liposomal structures (inset of Figure 1) are quite similar and do not report directly on the chromophore environment.

The fluorescence lifetime of Fluorazophore-L in homogeneous solution is similar to that of the parent compound, for example, 340 ns versus 325 ns in degassed *n*-hexane, respectively. In addition, the quenching rate constant, k_q , by α -Toc in benzene (3.9×10^9 M⁻¹ s⁻¹)⁵ is only slightly lower for Fluorazophore-L than for the parent (5.3×10^9 M⁻¹ s⁻¹),¹ which suggests a similar, essentially diffusion-controlled reactivity. In the lipidic assemblies and in the absence of quenchers, Fluorazophore-L shows monoexponential fluorescence decays with lifetimes (τ_0) of 140 ns in SDS micelles, 56 ns in Triton XR-100 micelles, and 116 ns in POPC liposome dispersions (error in lifetimes is ± 2 ns, all at 27 °C). They are shorter than the lifetime of DBO in neat aerated water ($\tau_0 = 325$ ns),¹ which can be ascribed to some quenching by the phospholipid or surfactant itself.^{5,29} In addition, the oxygen concentration may be higher in the lipidic self-assemblies than in bulk water.³⁰ The monoexponential decay behavior in the absence of quencher

- (18) Corkill, J. M.; Goodman, J. F.; Walker, T. *Trans. Faraday Soc.* **1967**, *63*, 768–772.
 (19) Barclay, L. R. C.; Locke, S. J.; MacNeil, J. M. *Can. J. Chem.* **1985**, *63*, 366–374.
 (20) Chiu, S. W.; Jakobsson, E.; Subramaniam, S.; Scott, H. L. *Biophys. J.* **1999**, *77*, 2462–2469.
 (21) Janczuk, B.; Bruque, J. M.; González-Martín, M. L.; Dorado-Calasanz, C. *Langmuir* **1995**, *11*, 4515–4518.
 (22) Calculations were carried out with HyperChem 5.0 (Hypercube Inc.).
 (23) Zeng, H.; Durocher, G. *J. Lumin.* **1995**, *63*, 75–84.
 (24) Capuzzi, G.; Lo Nostro, P.; Kulkarni, K.; Fernandez, J. E. *Langmuir* **1996**, *12*, 3957–3963.
 (25) Marquez, C.; Nau, W. M. *Angew. Chem., Int. Ed.* **2001**, *40*, 4387–4390.
 (26) Nau, W. M. *EPA Newsl.* **2000**, *70*, 6–29.

- (27) The parent DBO is too hydrophilic to undergo significant incorporation into micelles, which is reflected by the absence of solvatochromic shifts, cf.: Aikawa, M.; Yekta, A.; Liu, J.-M.; Turro, N. J. *Photochem. Photobiol.* **1980**, *32*, 297–303. This different behavior demonstrates that the palmitoyl chain in Fluorazophore-L is vital to promote efficient inclusion of the azo fluorophore into the lipidic nanoaggregates. Aikawa et al. exploited the propensity of hydrophilic azoalkanes to undergo a rapid exchange and distribution between micelles and water to study the fluorescence quenching of naphthalene in micelles. Note that the azoalkanes were employed as quenchers in this study.
 (28) Menger, F. M.; Doll, D. W. *J. Am. Chem. Soc.* **1984**, *106*, 1109–1113.
 (29) Nau, W. M.; Greiner, G.; Rau, H.; Wall, J.; Olivucci, M.; Scaiano, J. C. *J. Phys. Chem. A* **1999**, *103*, 1579–1584.
 (30) Dutta, A.; Popel, A. S. *J. Theor. Biol.* **1995**, *176*, 433–445.

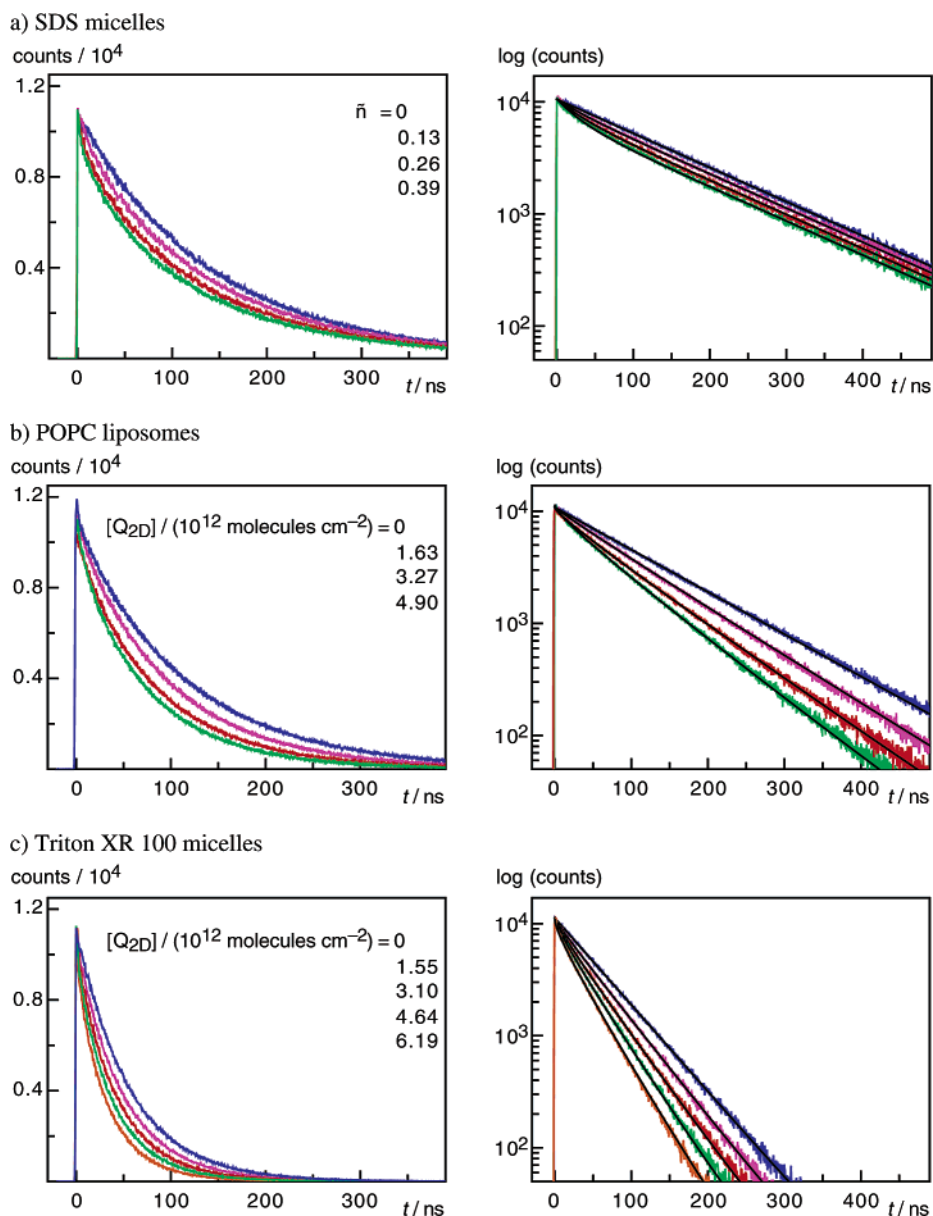


Figure 2. Linear (left) and semilogarithmic (right) plots of the Fluorazophore-L fluorescence decay with increasing concentration of α -Toc (from top to bottom) measured by single-photon counting in different lipidic assemblies: (a) in SDS (0.1 M) micelles, (b) in POPC (0.7 mM) liposomes, and (c) in Triton XR 100 (27 mM) micelles. The plots on the right include the respective global fitting curves (ideal micellar quenching model for SDS and 2D diffusion model for Triton and POPC).

and the fact that the lifetime was independent of the probe concentration clearly speak for a homogeneous distribution of probe molecules in the lipidic assemblies.⁵

Micelle and Liposome Size. In dynamic light-scattering experiments, the sizes (hydrodynamic radius) of the POPC liposomes (70 ± 3 nm) and Triton XR-100 micelles (4.0 ± 1.0 nm) were determined. They were found to be unaltered, within error, upon incorporation of Fluorazophore-L or α -Toc in the experimentally relevant concentration range (cf. Materials and Methods). The measured size of Triton XR-100 micelles coincides with that of unreduced Triton X-100 micelles (4.3 nm),³¹ by assuming a spherical shape. An oblate ellipsoid shape with radii of 5.2 and 2.7 nm³² is also discussed, but cannot be

readily distinguished. Recall that SDS micelles are too small (ca. 2 nm)³¹ to allow a reliable size determination by light scattering.

Quenching in SDS Micelles. Fluorescence quenching experiments with α -Toc in SDS micelles displayed a distinct non-monoexponential decay behavior. The semilogarithmic plots reveal an initial fast decay and a long-time monoexponential decay (Figure 2a). The latter is independent of the quencher concentration and remains parallel to the unquenched curve. This fluorescence decay behavior can be explained by the ideal micellar quenching model with a Poissonian-statistical distribution of quencher among the micelles,^{33,34} and which can be fitted according to eq 1.^{35–39} I_0 and $I(t)$ is the fluorescence intensity

(31) Maiti, N. C.; Krishna, M. M. G.; Britto, P. J.; Periasamy, N. *J. Phys. Chem. B* **1997**, *101*, 11051–11060.

(32) Robson, R. J.; Dennis, E. A. *J. Phys. Chem.* **1977**, *81*, 1075–1078.

(33) Infelta, P. P.; Grätzel, M.; Thomas, J. K. *J. Phys. Chem.* **1974**, *78*, 190–195.

(34) Turro, N. J.; Yekta, A. *J. Am. Chem. Soc.* **1978**, *100*, 5951–5952.

(35) Infelta, P. P. *Chem. Phys. Lett.* **1979**, *61*, 88–91.

at times 0 and t , and \bar{n} presents the average number of quenchers per micelle.

$$I(t) = I_0 \exp[-k_0 t - \bar{n}(1 - e^{-k_q' t})] \quad (1)$$

In micelles containing both an excited probe and one or more quencher molecules, a significant reduction of the fluorescence lifetime results (fast decay component), while micelles without quencher retain the original lifetime ($\tau_0 = 1/k_0$), which accounts for the distinct slow decay component. The quenching process in the small micellar volume (Figure 3a) can be approximated as a pseudo-first-order process with the rate constant being proportional to N , the number of quenchers per micelle,^{36,40} and k_q' , the characteristic quenching rate constant for a micelle with a single quencher. The bimodal decay pattern of the ideal micellar quenching model becomes most readily apparent at low quencher concentrations with less than one quencher per micelle on average ($\bar{n} < 1$, see below).³⁶ At these conditions, a significant number of micelles contain a probe but no quencher, which renders the characteristic slow decay component most pronounced (Figure 2a).

The unquenched fluorescence decay rate (k_0) was independent, within error, of the quencher concentration, which provides experimental evidence that no sizable intermicellar exchange of probe or quencher molecules occurs during the excited-state lifetime (immobile or stationary case). This, in fact, is the recommended condition for the determination of aggregation numbers according to eq 1 and can be ensured by the choice of low surfactant concentrations and water-insoluble probe and quencher, for example, Fluorazophore-L and α -Toc. The selection of a water-insoluble quencher allows also the simplified calculation of \bar{n} by the expression:

$$\bar{n} = \frac{[Q]N_s}{[\text{surf}] - \text{cmc}} \quad (2)$$

[Q] and [surf] denote the bulk quencher and bulk surfactant concentrations, which are experimentally adjusted. cmc is the critical micellar concentration,¹¹ and N_s presents the mean aggregation number, which is a fundamental size-related micelle parameter.

N_s can be extracted, along with k_q' , from time-resolved^{33,36,41} as well as steady-state^{34,35,42} fluorescence quenching experiments. As the assumptions made in time-resolved measurements are less restrictive,⁴¹ this method was preferred in the present study. For this purpose, the combined fluorescence decays at varying α -Toc concentrations were fitted (Figure 2a) with a global fitting routine according to the ideal micellar quenching model (eqs 1 and 2) to afford $N_s = 63 \pm 3$. The apparent unimolecular quenching rate constant (k_q') for an excited Fluorazophore-L probe by a single α -Toc quencher, both confined inside a SDS micelle composed of approximately 63 surfactant molecules, was found to be $2.4 \pm 0.4 \times 10^7 \text{ s}^{-1}$. It should also be noted that the global fitting according to

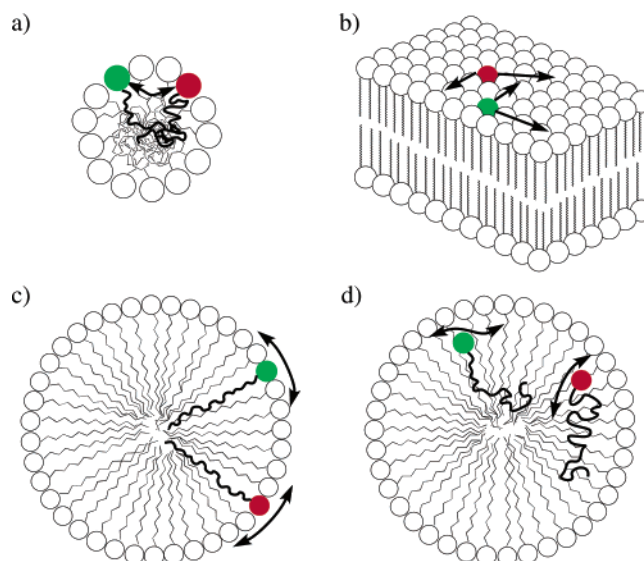


Figure 3. Presumed location and possible mode of diffusion of two amphiphilic reactants (a) in a small micelle, (b) in a lipid bilayer (2D), (c) in a larger micelle imposing 2D diffusion, and (d) in a larger micelle allowing 3D diffusion.

alternative quenching and diffusion models (see Triton and POPC data below) was not satisfactory for SDS micelles.

Quenching in POPC Liposomes. To study clearly defined vesicular structures and models for natural membranes, fluorescence quenching of Fluorazophore-L was investigated in fluid POPC liposomes. The injection method was chosen to obtain medium-sized single-shelled liposomes with a defined phospholipid/probe/quencher molar ratio and a narrow monomodal size distribution.^{13,14,16}

The diffusion of small molecules in membranes occurs predominantly in a lateral manner, that is, in two dimensions (2D) due to the small thickness of the bilayer. Lateral diffusion, as depicted in Figure 3b, is even more expected for amphiphilic reactants such as Fluorazophore-L and α -Toc. The fluorescence quenching in POPC liposomes presents therefore a case of a laterally diffusion-controlled reaction.⁴³ Fluorescence quenching in 2D was studied early by Razi Naqvi⁴⁴ and Owen,⁴⁵ who derived, on the basis of the fundamental work of Smoluchowski,⁴⁶ the relevant expression containing complex integrals of Bessel functions. The latter can be approximated^{45,47–49} by

(43) This assumption requires on one hand that the probe/quencher interaction is intrinsically diffusion-controlled, which is virtually fulfilled for the quenching of Fluorazophore-L by α -Toc in nonviscous organic solvents (compare bimolecular quenching rate constant in benzene of $3.9 \times 10^9 \text{ M}^{-1} \text{ s}^{-1}$), and the more expected in a viscous lipidic medium. In addition, the reactive groups of each reaction partner must be geometrically accessible, which is usually ensured through a similar transversal location and fulfilled for the Fluorazophore-L/ α -Toc system. Note that different transversal positions of the reactive groups are inconsistent with the Smoluchowski boundary condition for a 2D diffusion-controlled reaction, which imposes an instant reaction once the lateral distance between the reactants falls below a predefined reaction radius, cf. ref 46. Whenever the distance of the reactants does also depend on their transversal separation, the Collins–Kimball boundary condition has to be used (cf. ref 48 and Collins, F. C.; Kimball, G. E. *J. Colloid Sci.* **1949**, *4*, 425–437), which considers also the transversal motion (“bobbing up and down”) by assuming that the reaction occurs at a finite rate on encounter.

(44) Razi Naqvi, K. *Chem. Phys. Lett.* **1974**, *28*, 280–284.

(45) Owen, C. S. *J. Chem. Phys.* **1975**, *62*, 3204–3207.

(46) Von Smoluchowski, M. *Z. Phys. Chem.* **1917**, *92*, 129–168.

(47) Caruso, F.; Grieser, F.; Murphy, A.; Thistlethwaite, P.; Urquhart, R.; Almgren, M.; Wistus, E. *J. Am. Chem. Soc.* **1991**, *113*, 4838–4843.

(48) Medhage, B.; Almgren, M. *J. Fluoresc.* **1992**, *2*, 7–21.

(49) Razi Naqvi, K.; Martins, J.; Melo, E. *J. Phys. Chem. B* **2000**, *104*, 12035–12038.

(36) Almgren, M.; Löfroth, J.-E. *J. Colloid Interface Sci.* **1981**, *81*, 486–499.

(37) Miller, D. D.; Evans, D. F. *J. Phys. Chem.* **1989**, *93*, 323–333.

(38) Almgren, M. *Adv. Colloid Interface Sci.* **1992**, *41*, 9–32.

(39) Gehlen, M. H.; De Schryver, F. C. *Chem. Rev.* **1993**, *93*, 199–221.

(40) Van der Auweraer, M.; Dederen, J. C.; Geladé, E.; De Schryver, F. C. *J. Chem. Phys.* **1981**, *74*, 1140–1147.

(41) Alargova, R. G.; Kochijashky, I. I.; Sierra, M. L.; Zana, R. *Langmuir* **1998**, *14*, 5412–5418.

(42) Abuin, E.; Lissi, E. *Bol. Soc. Chil. Quím.* **1997**, *42*, 113–134.

employing the same functional form as for the exact decay law for fluorescence quenching in 3D systems (see below).⁴⁶ Razi Naqvi et al.⁴⁹ have recently demonstrated that the parameters used in eq 3 give very accurate results in most cases of practical interest and in particular for excited-state lifetimes (τ_0) around 100 ns. The 116-ns fluorescence lifetime of Fluorazophore-L in fluid POPC liposomes at 27 °C presents an ideal value in this respect, and we have therefore employed eq 3 to analyze the fluorescence decays.⁵⁰

$$I(t) = I_0 \exp[-(k_0 t + 2.31 D_L N_a [Q_{2D}] t + 7.61 \sqrt{D_L} R N_a [Q_{2D}] \sqrt{t})] \quad (3)$$

D_L in eq 3 represents the mutual lateral diffusion coefficient, R is the intermolecular distance at which quenching occurs, and $[Q_{2D}]$ is the two-dimensional quencher concentration on the lipid surface. The global fitting of the combined SPC data at different quencher concentrations (Figure 2b) affords $D_L = 1.8 \pm 0.1 \times 10^{-7} \text{ cm}^2 \text{ s}^{-1}$ and $R = 8.9 \pm 0.1 \text{ \AA}$, somewhat larger than the sum of the calculated van der Waals radii (7.3 \AA , see Materials and Methods). The short interaction radius determined from the experimental data is in line with hydrogen atom abstraction as the quenching mechanism between the singlet-excited azoalkane and the hydrogen donor α -Toc, that is, with an intimate probe/quencher contact.^{1,51,52}

Quenching in Triton XR-100 Micelles. The fluorescence quenching of Fluorazophore-L incorporated in Triton XR-100 micelles was markedly different from that observed in SDS micelles. The decays (Figure 2c) could not be fitted according to the ideal micellar quenching model (eq 1), the limitations of which are well known.^{40,53} Note, in particular, that the slope of the decays is strongly dependent on the quencher concentration even on long time scales.

The fluorescence quenching in the larger Triton micelles can be modeled either by assuming a diffusion of the reactive headgroups in a quasi-2D fashion along the surface of a spherical micelle (Figure 3c) or by a diffusion in three dimensions (3D) in a highly viscous homogeneous lipidic solution (Figure 3d).^{39,54,55} To the degree that Triton micelles can be viewed as microdroplets presenting small domains of homogeneous solutions, the fluorescence quenching can be analyzed as free diffusion in three dimensions (3D) in a viscous solution. To model this medium, the exact rate law for collision-induced intermolecular fluorescence quenching must be employed,^{45,46,56} that is, the Stern–Volmer expression has to be expanded by an additional square root term (eq 4). This term originates from the so-called diffusion depletion or transient effect, which is important to describe the initial period of the diffusion process until the diffusional steady-state is reached. A time-dependent quenching rate constant and deviations from monoexponential

decay behavior result, which become most significant in viscous solutions. Although not readily apparent from visual inspection alone, the decays in Figure 2b,c deviate significantly from monoexponentiality.

$$I_{(t)} = I_{(0)} \exp[-(k_0 t + k_V [Q_{3D}] t + k_D [Q_{3D}] \sqrt{t})] \quad (4)$$

with

$$k_V = 4\pi D R N_a \quad \text{and} \quad k_D = 8\sqrt{\pi D} R^2 N_a$$

k_V in eq 4 is a second-order quenching rate constant (in $\text{M}^{-1} \text{ s}^{-1}$), and k_D characterizes the diffusion depletion effect (in $\text{M}^{-1} \text{ s}^{-1/2}$). Both are functions of the mutual diffusion constant D and the reaction encounter distance R . The global data analysis of all decays for different α -Toc concentrations according to eq 4 yielded directly $D = 8.6 (\pm 0.2) \times 10^{-8} \text{ cm}^2 \text{ s}^{-1}$ and $R = 11.8 (\pm 0.2) \text{ \AA}$ for the 3D viscous-solvent diffusion model. An indirect data analysis according to eq 4 is outlined in the Supporting Information.

Alternatively, akin to the situation in liposomes, Fluorazophore-L and α -Toc may show a strong propensity to position their reactive dipolar headgroups at the micellar surface (Figure 3c). This location is supported by the solvatochromic shifts (see above). Quenching could entail a mutual lateral diffusion of the headgroups along the surface, which can be approximated, because the micelles are rather large, as a quasi-2D diffusion; that is, we ignore the surface curvature. The functional forms for the kinetics of fluorescence quenching in 2D and 3D are similar (eqs 3 and 4) and differ only by the factors and relative weights of R and D , and in the use of a 3D instead of a 2D concentration (see Materials and Methods). It is therefore not surprising that the Triton data can be equally well fitted according to the 2D diffusion/quenching model. The global fitting according to eq 3 yields $R = (8.0 \pm 0.2) \text{ \AA}$ and a lateral diffusion coefficient, D_L , of $3.5 (\pm 0.1) \times 10^{-7} \text{ cm}^2 \text{ s}^{-1}$.

A direct comparison of the 3D and 2D diffusion coefficients is not possible.^{38,57} However, the variations in the interaction radii and absolute magnitude of the diffusion coefficients can be used to evaluate which diffusion model is more suitable for the Triton micelles. Note, for example, that the 3D interaction radius of 11.8 \AA is considerably larger than the van der Waals contact distance of 7.3 \AA , and also larger than the value obtained in liposomes ($R = 8.9 \text{ \AA}$, see above). This deviation points to the use of an inappropriate diffusion model. Almgren, in particular, has suggested that a 3D analysis of a 2D diffusion system overestimates R (factor of 1.5 times too large) but underestimates the diffusion coefficient (factor of 3–6 too small).^{38,47} In fact, the 2D lateral diffusion model yields an interaction radius of 8.0 \AA , which is close to the anticipated one, and approximately a factor of 1.5 smaller than the 3D value. The 2D diffusion coefficient of $3.5 \times 10^{-7} \text{ cm}^2 \text{ s}^{-1}$ is 4 times larger than the one calculated by the 3D model, as projected by Almgren.³⁸

Data Treatment According to Stern–Volmer Quenching.

The rate constants and/or diffusion coefficients in the various lipidic assemblies as well as in benzene (for comparison) are presented in Table 1. Also included are additional results

(50) Caruso and coauthors, cf. ref 47, worked with air–water monolayers as a strictly 2D (flat) model system and proposed a similar parameter set optimized for shorter lifetimes ($\tau_0 < 5R^2/D_L$).

(51) Nau, W. M.; Greiner, G.; Rau, H.; Olivucci, M.; Robb, M. A. *Ber. Bunsen-Ges. Phys. Chem.* **1998**, *102*, 486–492.

(52) Sinicropi, A.; Pogni, R.; Basosi, R.; Robb, M. A.; Gramlich, G.; Nau, W. M.; Olivucci, M. *Angew. Chem., Int. Ed.* **2001**, *40*, 4185–4189.

(53) Tachiya, M. In *Kinetics of Nonhomogeneous Processes*; Freeman, G. R., Ed.; John Wiley & Sons: Chichester, 1987; pp 575–650.

(54) Hink, M. A.; van Hoek, A.; Visser, A. J. W. G. *Langmuir* **1999**, *15*, 992–997.

(55) Malliaris, A.; Le Moigne, J.; Sturm, J.; Zana, R. *J. Phys. Chem.* **1985**, *89*, 2709–2713.

(56) Nau, W. M.; Wang, X. *ChemPhysChem* **2002**, *3*, 393–398.

(57) Vanderkooi, J. M.; Fischkoff, S.; Andrich, M.; Podo, F.; Owen, C. S. *J. Chem. Phys.* **1975**, *63*, 3661–3666.

Table 1. Quenching Rate Constants and Mutual Diffusion Coefficients Obtained from the Fluorescence Quenching of Fluorazophore-L by α -Toc in Different Environments As Analyzed by Different Quenching Models (Recommended Values for Each Environment Are Bold)

environment	ideal micellar quenching ^a	lateral (2D) ^b	viscous (3D) ^c	nonviscous Stern–Volmer (3D) ^d	
	$k_q/10^7 \text{ s}^{-1}$	$D/10^{-7} \text{ cm}^2 \text{ s}^{-1}$	$D/10^{-7} \text{ cm}^2 \text{ s}^{-1}$	$k_q/10^8 \text{ M}^{-1} \text{ s}^{-1}$	$D/10^{-7} \text{ cm}^2 \text{ s}^{-1}$ ^e
benzene				39 ± 2	≥70 ^f
SDS micelles	2.4 ± 0.4^g			~3.8	~6.9
POPC liposomes		1.8 ± 0.1^h		0.84 ± 0.02	~1.5
Triton micelles		3.5 ± 0.1ⁱ	0.86 ± 0.02 ^j	1.4 ± 0.1	~2.4 ^k

^a From fitting according to eqs 1 and 2. ^b From fitting according to eq 3. ^c From fitting according to eq 4. ^d Classical Stern–Volmer treatment with 3D concentrations, see Supporting Information. ^e Obtained with the relationship for a diffusion-controlled reaction in a nonviscous solvent, that is, $k_q \equiv k_{\text{diff}} = 4\pi N_a R D$, by assuming the van der Waals distance (7.3 Å) as the interaction radius as well as a unit quenching efficiency. ^f Lower limit due to the assumption of unit quenching efficiency. ^g $N_s = 63 \pm 3$. ^h $R = 8.9 \pm 0.1$ Å; see Supporting Information for the results obtained from various approximations based on monoexponential fitting. ⁱ $R = 8.0 \pm 0.2$ Å. ^j $R = 11.8 \pm 0.2$ Å; the fitting according to an approximate linear regression method as described in refs 37, 101, cf. Supporting Information, provides $D = 9.8 (\pm 4.1) \times 10^{-8} \text{ cm}^2 \text{ s}^{-1}$ and $R = 11.0 \pm 3.6$ Å. ^k The large deviation as compared to the 3D value for viscous solvents (see same entry on left) is due to the fixed radius in the fitting procedure.

obtained from several more approximate analytical procedures, which are outlined in the Supporting Information. In particular, it should be noted that the fluorescence quenching can be crudely treated in a simple Stern–Volmer manner to allow a comparison of the largely different environments. This affords estimates of the apparent bimolecular quenching rate constants (k_q) and the mutual diffusion coefficients (Table 1) with the order benzene \gg SDS > Triton X-100 > POPC. This trend can be understood in terms of pronounced variations in (micro)viscosity.^{31,36,54,58} Expectedly, diffusion in benzene occurs more than 1 order of magnitude faster than in the more viscous lipidic assemblies.

Discussion

The main physiological function of the antioxidant α -Toc is the scavenging of chain-propagating lipid peroxy radicals to inhibit lipid peroxidation. The antioxidant function derives from the phenolic hydroxyl group in the chromanol headgroup that can donate its weakly bound hydrogen atom. In heterogeneous membrane systems, α -Toc owes its antioxidant potency also to its accessibility within the membrane as well as from the aqueous bulk.⁵⁹ From independent experiments including IR and Raman spectroscopy,⁶⁰ EPR with nitroxides as spin probes,⁶¹ NMR techniques,⁷ and intrinsic α -Toc fluorescence,^{62–64} it has been concluded that α -Toc has its phytyl tail in the hydrophobic core and its chromanol group located near the polar moiety of the lipid, that is, at the water–lipid interface. In fact, this is the region of interest with respect to its antioxidant action, because it is the presumed position of polar peroxy radicals as well.⁶⁵ Consider Scheme 2, which presents an illustration⁶⁶ of a presumed antioxidant cycle of α -Toc scavenging a lipid peroxy radical in a membrane.^{67,68}

To model the antioxidant activity of α -Toc in membranes, low-density lipoprotein (LDL),^{69–71} and other lipidic and heterogeneous systems of biological or food industry-related

interest, it is fundamental to understand the diffusional behavior of this antioxidant. This comprises knowledge of the most appropriate diffusion models and the derived diffusion coefficients. Relatively little is known about the diffusional properties of α -Toc in lipid microcompartments, which has motivated the present study in SDS and Triton micelles as well as in POPC liposomes.

Conceptual Approach. A suitable direct method to monitor the diffusion of α -Toc in membrane models involves the instantaneous generation, for example, by a laser pulse, and time-resolved spectroscopic observation of a reactive species, which is being scavenged by the antioxidant. Presently, we have employed the lipid-soluble Fluorazophore-L, which serves as a fluorescent probe for antioxidant activity by mimicking reactive peroxy and alkoxy radicals.^{1,3} The fluorescence of the azo chromophore is quenched by antioxidants such as α -Toc at a diffusion-controlled rate, such that the kinetics of fluorescence quenching reports directly on the mobility or the (local) concentration of the antioxidant. Because lateral diffusion is assumed to be the rate-limiting step for the interception of reactive lipid radicals in membranes, Fluorazophore-L should allow the investigation of this essential reaction step (compare Schemes 2 and 3). The quenching mechanism is hydrogen abstraction, which requires an intimate contact of the azo group and the phenolic hydroxyl moiety.^{1,51,52}

The most important property of Fluorazophore-L is its long fluorescence lifetime in micelles and liposomes (ca. 50–150 ns). The study of intermolecular reaction dynamics in lipidic heterogeneous assemblies by the probe/quencher methodology requires such very long-lived luminescent probes to allow the slow diffusion of probe and quencher (submicrosecond time scale) in the viscous environment to compete with the intrinsic excited-state decay.^{15,56,72,73} This allows the observation of

(58) Zana, R. *J. Phys. Chem. B* **1999**, *103*, 9117–9125.

(59) Packer, L. In *Bioradicals Detected by ESR Spectroscopy*; Ohya-Nishiguchi, H., Packer, L., Eds.; Birkhäuser Verlag: Basel, Switzerland, 1995; pp 237–257.

(60) Lefevre, T.; Picquart, M. *Biospectroscopy* **1996**, *2*, 391–403.

(61) Takahashi, M.; Tsuchiya, J.; Niki, E. *J. Am. Chem. Soc.* **1989**, *111*, 6350–6353.

(62) Aranda, F. J.; Coutinho, A.; Berberan-Santos, M. N.; Prieto, M. J. E.; Gomez-Fernandez, J. C. *Biochim. Biophys. Acta* **1989**, *985*, 26–32.

(63) Gómez-Fernández, J. C.; Aranda, F. J.; Villalafín, J. In *Progress in Membrane Biotechnology*; Gómez-Fernández, J. C., Chapman, D., Packer, L., Eds.; Birkhäuser Verlag: Basel, Switzerland, 1991; pp 98–117.

(64) Fukuzawa, K.; Ikebata, W.; Sohmi, K. *J. Nutr. Sci. Vitaminol.* **1993**, *39*, S9–S22.

(65) Barclay, L. R. C.; Ingold, K. U. *J. Am. Chem. Soc.* **1981**, *103*, 6478–6485.

(66) The initially formed radical undergoes rearrangement (cf.: Brash, A. R. *Lipids* **2000**, *35*, 947–952. Porter, N. A.; Wujek, D. G. *J. Am. Chem. Soc.* **1984**, *106*, 2626–2629) which is not shown in detail in Scheme 2. Scheme 2 allows also for a possible interception of peroxy radicals by vitamin C. This interception by ascorbate is less efficient than that by α -tocopherol (cf. Doba, T.; Burton, G. W.; Ingold, K. U. *Biochim. Biophys. Acta* **1985**, *835*, 298–303. Niki, E.; Kawakami, A.; Yamamoto, Y.; Kamiya, Y. *Bull. Chem. Soc. Jpn.* **1985**, *58*, 1971–1975), but may become sizable in special cases, for example, at low pH, cf. ref 6.

(67) Barclay, L. R. C. *Can. J. Chem.* **1993**, *71*, 1–16.

(68) Buettner, G. R. *Arch. Biochem. Biophys.* **1993**, *300*, 535–543.

(69) Noguchi, N.; Niki, E. *Free Radical Res.* **1998**, *28*, 561–572.

(70) Bowry, V. W.; Ingold, K. U. *Acc. Chem. Res.* **1999**, *32*, 27–34.

(71) Alessi, M.; Paul, T.; Scaiano, J. C.; Ingold, K. U. *J. Am. Chem. Soc.* **2002**, *124*, 6957–6965.

(72) Davenport, L.; Targowski, P. *J. Fluoresc.* **1995**, *5*, 9–18.

(73) Kusba, J.; Li, L.; Gryczynski, I.; Piszczek, G.; Johnson, M.; Lakowicz, J. R. *Biophys. J.* **2002**, *82*, 1358–1372.

example, of rhenium(I)⁷⁵ and ruthenium(III),⁷⁶ as large chromophores. The combination of a simple headgroup/tail topology, the nonaromatic uncharged fluorescent headgroup, and the long fluorescence lifetime render Fluorazophore-L unique among previously investigated probes and, because of the small fluorophore, presumably less invasive toward the structures of monolayers, liposomes, and micelles.^{5,54} In contrast to the alternative chromophores, the fluorescence of Fluorazophore-L remains also long-lived in aerated aqueous solution due to inefficient oxygen quenching,^{26,77} which bypasses the need for special degassing procedures. Finally, the azo chromophore does not tend to form concentration-dependent excimers or ground-state aggregates as polycyclic aromatic chromophores do, which simplifies the analysis of the quenching kinetics. The long fluorescence lifetime of Fluorazophore-L, however, comes at the expense of a very low extinction coefficient, both of which are directly related to the orbital-forbidden nature of the underlying $n \rightarrow \pi^*$ electronic transition;²⁶ the latter precludes one to achieve, unfortunately, single molecule sensitivity during fluorescence detection.^{77,78}

Fluorazophore-L bears a palmitoyl chain, which is expected to be immersed in the hydrophobic core of micelles and lipid bilayers, while the polar and reactive headgroup (dipole moment ca. 3.2 and 3.5 D for the singlet-excited⁷⁹ and ground-state⁸⁰ chromophore) is positioned close to the lipid/water interface. This should allow for an efficient spatial interaction with the chromanol headgroup of α -Toc (dipole moment ca. 2.9 D)⁸¹ as illustrated in Scheme 3. The position of the azo chromophore mimics the presumed location of the reactive group of lipid peroxy radicals. In essence, Fluorazophore-L takes over the role of the polar peroxy radicals (compare Schemes 2 and 3), and, instead of monitoring the interaction of a radical with the antioxidant, we employ an excited state as a probe because its fluorescence response can be directly temporally resolved.

The amphiphilic Fluorazophore-L has already been successfully employed in micelles and liposomes to monitor quenching by the water-soluble ascorbic acid (k_{AA} in Scheme 3) and to determine the related pH-dependent kinetics.⁶ The observed efficient interaction with ascorbic acid, the solvatochromic shifts (cf. Results), as well as surface pressure–area (π – A) measurements in air–water monolayers⁵ provide strong experimental support that the reactive azo chromophore resides at the lipid/water interface as shown in Schemes 1 and 3. This position is identical to that of α -Toc, which is also known to react (as tocopheroxyl radical) with ascorbate in the same compartmental region (k_{AA} in Scheme 2).^{7,64,68,82,83} Because the reactive groups in α -Toc and in Fluorazophore-L are both accessible from the aqueous bulk, their position within a lipid assembly must be similar, which meets an important nontrivial prerequisite of our

conceptual approach. In addition, it should be mentioned that the lipophilicity of Fluorazophore-L, like that of α -Toc,^{71,84} is sufficiently high to disregard an interparticle lipid exchange or a partitioning into the aqueous phase.²⁷ The lipophilicity is born out, among others, in Langmuir monolayer experiments.⁵ The probe/quencher pair Fluorazophore-L/ α -Toc stands therefore for an immobile or stationary case; that is, no migration between the surfactant or lipid bilayer assemblies takes place within the excited-state lifetime. This situation allows for a more rigorous analysis of the transient decay data.³⁶

Diffusion Models. Several models have been developed to analyze diffusion-controlled reactions and in particular excited-state quenching in micellar and vesicular environments. The choice of the appropriate model depends on the properties of probe and quencher and the type and size of the lipidic assembly. In ambiguous cases, qualitative or quantitative discrepancies of the diffusion parameters need to be used to identify the most suitable model.

Qualitatively, micelles and vesicles with stationary probes and quenchers have been proposed to exhibit a distinct time-resolved quenching behavior, which is signaled, among others, by the shapes of their respective semilogarithmic decay curves.³⁷ This marked difference is also manifested in the decays related to fluorescence quenching of Fluorazophore-L by α -Toc (Figure 2). In the case of Triton micelles and POPC liposomes, the slopes of fluorescence decays are nonmonoexponential and strongly concentration-dependent. For SDS micelles, on the other hand, there is an initial fast decay component and a monoexponential decay on longer time scales, which is independent of quencher concentration.

Quenching in SDS Micelles. The fluorescence quenching behavior of Fluorazophore-L by α -Toc in SDS micelles (see Figure 2a) can be well described by the ideal micellar quenching model, in which each micelle is considered as a very small reaction vessel containing a discrete number of 0, 1, 2, 3, etc. quencher molecules distributed in a Poissonian manner. Due to the small molecular dimensions of the micellar reaction containers, only short-distance diffusion is required, which can be described by a quasi-unimolecular intramicellar quenching rate constant, akin to the pseudo-unimolecular quenching of an excited state by a solvent. The pertinent analysis according to eq 1 affords the mean aggregation number (N_s). While N_s may vary due to the total surfactant concentration,⁴¹ temperature,^{55,85} and the type and concentration of ionic,³⁴ or organic additives,¹¹ the value of N_s measured for SDS in the present study (63 ± 3) falls within the range of reported values (57–76).^{11,39,41,85–87} The apparent unimolecular rate constant (k_q') for fluorescence quenching of Fluorazophore-L and α -Toc in SDS micelles with a single quencher was found to be $2.4 (\pm 0.4) \times 10^7 \text{ s}^{-1}$. This value is slightly lower than rates constants reported for pyrene/hexadecylpyridinium chloride ($3.4 \times 10^7 \text{ s}^{-1}$)⁴¹ or 1-methylpyrene/*N*-tetradecylpyridinium chloride ($3.5 \times 10^7 \text{ s}^{-1}$).⁸⁸ For these alternative systems, it has to be taken into account that the probe (pyrene) does not contain a lipophilic tail and is

(74) Martins, J.; Vaz, W. L. C.; Melo, E. *J. Phys. Chem.* **1996**, *100*, 1889–1895.

(75) Guo, X.-Q.; Castellano, F. N.; Li, L.; Szmecinski, H.; Lakowicz, J. R.; Sipior, J. *Anal. Biochem.* **1997**, *254*, 179–186.

(76) Hackett, J. W., II; Turro, C. J. *Phys. Chem. A* **1998**, *102*, 5728–5733.

(77) Hudgins, R. R.; Huang, F.; Gramlich, G.; Nau, W. M. *J. Am. Chem. Soc.* **2002**, *124*, 556–564.

(78) Neuweiler, H.; Schulz, A.; Böhmer, M.; Enderlein, J.; Sauer, M. *J. Am. Chem. Soc.* **2003**, *125*, 5324–53330.

(79) Nau, W. M.; Pischel, U. *Angew. Chem., Int. Ed.* **1999**, *38*, 2885–2888.

(80) Harmony, M. D.; Talkington, T. L.; Nandi, R. N. *J. Mol. Struct.* **1984**, *125*, 125–130.

(81) Babu, K.; Gadre, S. R. *J. Comput. Chem.* **2003**, *24*, 484–495.

(82) Bisby, R. H.; Ahmed, S. *Free Radical Biol. Med.* **1989**, *6*, 231–239.

(83) Bisby, R. H.; Parker, A. W. *Arch. Biochem. Biophys.* **1995**, *317*, 170–178.

(84) Castle, L.; Perkins, M. J. *J. Am. Chem. Soc.* **1986**, *108*, 6381–6382.

(85) Shah, S. S.; Jamroz, N. U.; Sharif, Q. M. *Colloids Surf., A* **2001**, *178*, 199–206.

(86) Iglesias, E.; Montenegro, L. *Phys. Chem. Chem. Phys.* **1999**, *1*, 4865–4874.

(87) Bockstahl, F.; Duplâtre, G. *Phys. Chem. Chem. Phys.* **2000**, *2*, 2401–2405.

(88) Boens, N.; Luo, H.; van der Auweraer, M.; Reekmans, S.; de Schryver, F. C.; Malliaris, A. *Chem. Phys. Lett.* **1988**, *146*, 337–342.

therefore presumably less confined within the micelle than an amphiphilic reactant.

Lateral Diffusion in POPC Liposomes. Diffusion and therefore fluorescence quenching in liposomes is presumed to occur in a lateral fashion along a leaflet with retention of the relative transversal position of the tail and headgroup (Figure 3b). Most importantly, while for highly viscous 3D systems a diffusional steady-state is rapidly established after an initial period of time, this is not the case in a 2D system, where a time-independent bimolecular rate “constant” can never be attained for theoretical reasons.^{45,47,56,74} The liposome decay data were analyzed according to the formula of Razi Naqvi et al.⁴⁹ in eq 3 and afforded a mutual lateral diffusion coefficient (D_L) of $1.8 (\pm 0.1) \times 10^{-7} \text{ cm}^2 \text{ s}^{-1}$ at 27 °C. The mutual diffusion coefficient is the sum of the individual diffusion coefficients, thereby providing an upper limit for the individual ones. The sizes of probe and quencher are very similar for Fluorazophore-L and α -Toc, and both bear a single lipid tail, such that we can estimate a diffusion coefficient of $9 \times 10^{-8} \text{ cm}^2 \text{ s}^{-1}$ for α -Toc alone, one-half of the mutual diffusion coefficient.

Knowledge of the lateral diffusion coefficient of α -Toc in membrane models is invaluable for the understanding of its natural antioxidant activity (Scheme 2), because the rate of diffusion sets an upper limit to the scavenging rate of reactive radicals. In this context, Aranda et al. proposed that the high antioxidant efficiency of α -Toc is due to its exceptionally high lateral mobility in membranes, as implied by the 50-times larger diffusion coefficient obtained in their work ($4.8 \times 10^{-6} \text{ cm}^2 \text{ s}^{-1}$).⁶² The latter value was derived from the steady-state fluorescence quenching of α -Toc itself by the paramagnetic 5-doxylstearate in egg yolk phosphocholine liposomes, which should be comparable (e.g., with respect to the lipid composition and phase at ambient temperature) to POPC liposomes. In short, the method used in the previous study is unlikely to provide reliable data because it is based on an apparent bimolecular quenching rate obtained from modified Stern–Volmer plots by using three-dimensional concentrations, by allowing for a partitioning between water and lipid, by assuming an isotropic diffusion of spherical reactants, and by applying a potentially inappropriate combination of analytical procedures,^{89–91} which has already been critically discussed by others.⁹² The failure of the method based on the intrinsic α -Toc fluorescence can be simply rationalized: The fluorescence lifetime of α -Toc is far too short ($< 2 \text{ ns}$ in phosphocholine liposomes)^{82,93} to report reliably on diffusional phenomena in the viscous membrane environment. The time scale of diffusion in membrane models is much slower, in the range of several hundred nanoseconds (Figure 2), such that long-lifetime probes are indispensable to obtain sizable quenching effects and therefore accurate data.

While our present data contrast the results from Aranda et al., they demonstrate that the individual lateral diffusion coefficient of α -Toc lies with ca. $9 \times 10^{-8} \text{ cm}^2 \text{ s}^{-1}$ well in the range of other lipids in fluid phospholipid membranes ($D_L \approx 10^{-8}–10^{-7} \text{ cm}^2 \text{ s}^{-1}$).^{94,95} For example, the lateral diffusion coefficient of POPC itself has been reported to be $4.2–4.7 \times$

$10^{-8} \text{ cm}^2 \text{ s}^{-1}$.^{96–98} This means that α -Toc does not diffuse particularly rapidly, although it may diffuse about a factor of 2 faster than phospholipids, presumably as a consequence of its smaller molecular size and the single lipid chain.⁹⁵ Note, in this context, that most previously reported lateral diffusion coefficients have been obtained by alternative techniques such as excimer fluorescence,⁷⁴ fluorescence recovering after photobleaching (FRAP),^{94,96} single-particle tracking,^{97,99} and fluorescence correlation spectroscopy.¹⁰⁰ These are generally inapplicable to natural membrane constituents without chemical modification, that is, fluorophore labeling. The advantage of the present probe/quencher technique, while indirect because it is based on the fluorescence quenching of Fluorazophore-L, is that it allows the study of the diffusional properties of chemically unmodified α -Toc.

Quenching in Triton Micelles. The measurements in relatively small SDS micelles with anionic headgroups (radius ca. 2 nm) and in POPC liposomes (radius 70 nm) were compared to the decay in Triton XR-100 micelles, which have nonionic headgroups, a quite polar polyoxyethylene shell, and a radius of ca. 4 nm. As becomes evident from the fluorescence decay traces (Figure 2), Triton micelles are sufficiently different from SDS micelles⁵⁴ to cause a break-down of the ideal micellar quenching model. In fact, the qualitative appearance of the fluorescence decays in Triton micelles is more reminiscent of those in liposomes. The decays can be fitted by treating the reaction as either a 2D quenching process originating from a lateral diffusion of the probe and quencher along the surface of the micellar sphere (Figure 3c) or, alternatively, as quenching in a viscous 3D medium with each Triton micelle presenting a microdroplet of a homogeneous solution (Figure 3d).^{39,54,55} The better agreement of the fitted parameters obtained from the 2D as opposed to a 3D diffusion model (cf. Results) leads us to suggest that the mutual diffusion of Fluorazophore-L and α -Toc in the medium-sized Triton XR-100 micelles can be well described as being 2D-lateral in nature (“surface diffusion”, Figure 3c). This is in line with a preferential intramicellar orientation of α -Toc (and Fluorazophore-L) similar to that found in bilayer membranes, that is, with the polar reactive headgroups located at the micelle–water interface. A preferential diffusion along the surface of Triton micelles has also been suggested in previous studies.^{31,54} The 2D lateral diffusion model yields an interaction radius of 8.0 Å and a mutual 2D diffusion coefficient of $3.5 \times 10^{-7} \text{ cm}^2 \text{ s}^{-1}$. Note that the latter value is about twice as large as that for POPC liposomes, which is expected due to the looser lipid packing in the less structured micelles.⁵⁴

(89) Lakowicz, J. R.; Hogen, D. *Chem. Phys. Lipids* **1980**, *26*, 1–40.

(90) Umberger, J. Q.; LaMer, V. K. *J. Am. Chem. Soc.* **1945**, *67*, 1099–1109.

(91) Fato, R.; Battino, M.; Esposti, M. D.; Castelli, G. P.; Lenaz, G. *Biochemistry* **1986**, *25*, 3378–3390.

(92) Rajarathnam, K.; Hochman, J.; Schindler, M.; Ferguson-Miller, S. *Biochemistry* **1989**, *28*, 3168–3176.

(93) Sow, M.; Durocher, G. *J. Photochem. Photobiol., A* **1990**, *54*, 349–365.

(94) Van der Meer, B. W. In *Biomembranes: Physical Aspects*; Shinitzky, M., Ed.; VCH: Weinheim, 1993; pp 97–158.

(95) Johnson, M. E.; Berk, D. A.; Blankschtein, D.; Golan, D. E.; Jain, R. K.; Langer, R. S. *Biophys. J.* **1996**, *71*, 2656–2668.

(96) Vaz, W. L. C.; Clegg, R. M.; Hallmann, D. *Biochemistry* **1985**, *24*, 781–786.

(97) Schütz, G. J.; Schindler, H.; Schmidt, T. *Biophys. J.* **1997**, *73*, 1073–1080.

(98) Böckmann, R. A.; Hac, A.; Heimbürg, T.; Grubmüller, H. *Biophys. J.* **2003**, *85*, 1647–1655.

(99) Eggeling, C.; Widengren, J.; Rigler, R.; Seidel, C. A. M. In *Applied Fluorescence in Chemistry, Biology and Medicine*; Rettig, W., Strehmel, B., Schrader, S., Seifert, H., Eds.; Springer-Verlag: Berlin, 1999; pp 193–240.

(100) Hink, M.; Visser, A. J. W. G. In *Applied Fluorescence in Chemistry, Biology and Medicine*; Rettig, W., Strehmel, B., Schrader, S., Seifert, H., Eds.; Springer-Verlag: Berlin, 1999; pp 101–118.

(101) Miller, D. D.; Magid, L. J.; Evans, D. F. *J. Phys. Chem.* **1990**, *94*, 5921–5930.

Relative Antioxidant Activity of α -Toc in Different Lipidic Assemblies. The rate by which α -Toc can intercept reactive radicals will markedly depend on the microviscosity of the lipid. In our set of experimental data with the radical mimic Fluorazophore-L, this is borne out by the faster reaction rates and higher diffusion coefficients, which follow the order benzene \gg SDS > Triton XR-100 > POPC (Table 1). However, the net efficiency by which all reactive radicals are removed from the system is not only dependent on the rate, but also on the availability of antioxidant in the lipidic assembly. In particular, if the size of the assemblies becomes sufficiently small and if interparticle exchange is slow, there is a probability that some assemblies (at a given concentration) no longer contain an antioxidant molecule any more, such that many reactive radicals could survive even if the intrinsic rate of scavenging by an antioxidant is high. Exactly this is the case for SDS micelles, which show the largest rate constants and diffusion coefficients for α -Toc, but for which nevertheless the amount of unscavenged radicals (mimicked in our experiments through the survival of excited Fluorazophore-L) is large because some SDS micelles contain no antioxidant for statistical reasons. This becomes apparent from the inspection of the fluorescence decay curves in Figure 2, which refer to comparable ranges of three-dimensional concentrations ($[Q_{3D}]$ up to 25 mM for SDS, 45 mM for POPC, and 81 mM for Triton XR-100). The integrals under the curves in the presence of α -Toc, which are a measure of the surviving reactive excited states, are larger for SDS than for POPC liposomes regardless of the intrinsically higher quenching rate constant (Table 1). A relatively low antioxidant activity of α -Toc in SDS micelles has already been proposed previously.⁸⁴ This means that the size of the lipidic assembly may become in special cases a more important parameter for the net antioxidant activity than the diffusion coefficient. Our results support the suggestion that very small lipidic assemblies, as for example LDL particles, are prime targets for lipid peroxidation^{70,71} and may even serve as a reservoir of reactive radicals.

Conclusions

Fluorazophore-L has been established as an amphiphilic fluorescent probe for the investigation of antioxidant activity in model membrane systems. While a previous study has dealt with the interfacial reactivity toward the water-soluble ascorbic acid (vitamin C), the present study has focused on the fluorescence quenching by the lipid-soluble α -Toc (the most active component of vitamin E). This study has provided the first direct spectroscopic and real time-resolved data for the reaction of α -Toc with a reactive intermediate in a membrane model. The experimental data allow one to draw conclusions on the diffusion behavior of this important antioxidant in

different lipidic assemblies. Accordingly, the quenching by α -Toc in SDS micelles obeys the ideal micellar quenching model, which is based on a Poissonian quencher distribution and affords a quasi-unimolecular rate constant. In contrast, fluorescence quenching in the larger Triton XR-100 micelles can be best modeled by assuming a lateral diffusive motion of the amphiphilic antioxidants along the micellar surfaces. The quenching behavior in POPC liposomes is also consistent with a lateral diffusion and has allowed an estimate of $9 \times 10^{-8} \text{ cm}^2 \text{ s}^{-1}$ for the lateral diffusion coefficient of α -Toc in these model membrane systems. This is an important benchmark value for modeling the antioxidant (as well as prooxidant)^{65,69,70} activity of the lipophilic α -Toc in biological membranes and other heterogeneous systems⁸⁴ of interest in biology and food industry, especially because there is a current interest in its action and diffusion in LDL particles.⁷¹ The measured mutual diffusion coefficient allows one to predict an upper limit for the rate by which vitamin E can scavenge lipid peroxy radicals. Noteworthy, a simple time-independent diffusion-limited rate constant cannot be provided for α -Toc in membranes due to the complexity of the expected reaction kinetics (eq 3), which leads to a time-dependent rate constant at all times. It is important to note, and in contrast with previous studies,⁶² that we have obtained no experimental indication of an extraordinarily fast diffusion of α -Toc in any of the lipidic assemblies. The high antioxidant activity of vitamin E should therefore be accounted for by its intrinsically high hydrogen donor activity and its favorable location within bilayer membranes, and not by a particularly fast diffusion. In summary, the present investigations allow a better quantitative understanding of the diffusion of α -Toc, which is fundamental for modeling and understanding oxidative-stress related processes such as lipid peroxidation (see Scheme 2).

Acknowledgment. This work was supported by the Swiss National Science Foundation (MHV grant 2134-62567.00 for G.G., NF grant 620-58000.99 for W.M.N.). The study was performed within the Swiss National Research Program "Supramolecular Functional Materials" (grant 4047-057552 for W.M.N.). We are very thankful to Prof. W. Meier and his group for fruitful discussions as well as for performing the light-scattering experiments, and we thank Prof. M. Winterhalter for his comments. We are also very grateful to A. Sonnen for his help with the SDS quenching experiments.

Supporting Information Available: Approximate analytical procedures to treat the fluorescence quenching in micelles and liposomes (PDF). This material is available free of charge via the Internet at <http://pubs.acs.org>.

JA039845B